ELSEVIER

Coordination Chemistry Reviews
159 (1997) 135–151

COORDINATION CHEMISTRY REVIEWS

Photochemistry as a tool for elucidating organometallic reaction mechanisms

William Boese, Karen McFarlane, Brian Lee, Julie Rabor, Peter C. Ford *

Department of Chemistry, University of California, Santa Barbara, CA 93106, USA

Received 22 December 1995

Contents

Abstract

This paper reviews recent studies in these laboratories in which laser flash photolysis with time-resolved IR and optical detection was used to probe the reactivities and structures of intermediates relevant to the catalytic activation of carbon monoxide. Of particular interest are mechanisms of the carbonylations of metal–alkyl bonds. Summarized here are studies of the model systems $(\eta^5\text{-}C_5H_5)Fe(CO)_2(COCH_3)$ and $Mn(CO)_5(COCH_3)$ as well as initial investigations on the catalytic species $Co(CO)_3(PPh_3)(COCH_3)$. © 1997 Elsevier Science S.A.

Keywords: Photochemistry; Organometallic reaction mechanisms

* Corresponding author.

PII S0010-8545(96)01309-4

1. Introduction

Important reactions in organometallic chemistry that have been the focus of many mechanistic studies include the activation of C–H and H–H bonds, ligand substitution reactions, and other processes relevant to catalytic and photocatalytic activation of small molecules such as carbon monoxide [1,2]. A major problem in elucidating the detailed mechanisms is to characterize the structures and reactivities of intermediates formed along reaction coordinates. Such transient species are elusive under thermal catalytic (or stoichiometric) conditions owing to the low steady-state concentrations which impede direct spectroscopic (and other) observation. Other conditions and methods must be used, meanwhile ensuring that the high energy species studied are those of interest in the thermal reaction schemes. To this end, flash photolysis can be a tool for preparing high, non-steady-state concentrations of reaction intermediates [1,3–8]. The natures of such species are interrogated with time-resolved optical (TRO) or infrared (TRIR) spectroscopic detection to provide an ensemble of spectroscopic and kinetic information to enable the elucidation of their structures and reactivities.Infrared detection is particularly useful for spectroscopic characterization and kinetic studies of the reactants, intermediates, and products of certain organometallic reactions, especially if the relevant compounds include groups which have strong absorption bands. The broad, often featureless, UV-Vis absorption bands common to many organometallic compounds in solution generally allow little structural interpretation, and the absorption bands of the various species in solution often overlap. The much sharper IR bands give better resolution between individual species, and can be probed either by time-resolved laser flash photolytic experiments at ambient temperature or by FTIR under low temperature conditions where subsequent reactions of the transients are extremely slow. Carbonyl stretching bands generally have high extinction coefficients and are relatively narrow. Numerous qualitative and quantitative criteria have been elaborated for the analysis of such bands in terms of structure and bonding around the metal center, and the narrow bands often allow for direct observation of the temporal decay and appearance of individual species without interference from excessive overlapping.The TRO and TRIR instruments used for the collection of the data for the investigations summarized below have been described previously [9,10] with modifications in sample handling [10].A mechanism which has attracted the attention of this group has been the formation of carbon–carbon bonds via CO "migratory insertion" into metal alkyl bonds (Eq. (1)). The interest in this extensively investigated fundamental reaction draws in large part from its proposed roles in various catalytic schemes, such as methanol carbonylation to acetic acid, alkene hydroformylation, etc. [11]. Characterizing the structure and reactivity of intermediate $\mathbf{I}_{th}$ has been a major challenge [12].

Thermal reactions of the prototypes $Mn(CO)_5R$ and $CpFe(CO)_2R$ ($Cp = \eta^5$-C_5H_5) have been studied extensively as models for migratory insertion [13–28]. The strategy used in this laboratory to address the formation of intermediates involves the preparation of relevant key intermediates by photolytic decarbonylation of the metal acetyl to form the "coordinatively unsaturated" transient species **I**. The

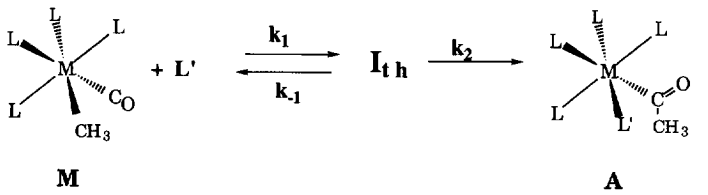

M A (1)

reverse of Eq. (1), i.e., alkyl migration to form the metal alkyl (Eq. (2)) and competitive trapping by CO or other ligands are then monitored.

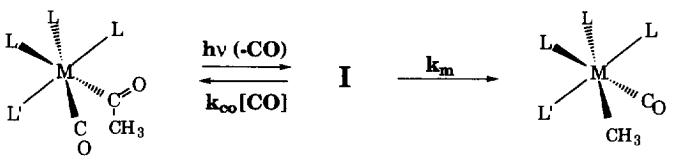

A M (2)

The resulting TRO and TRIR spectra as well as the reaction dynamics of the systems under various conditions are then interpreted in terms of potential mechanisms. Comparisons of rates obtained in this manner to the competitive reactivities deduced for I_{th} based upon the application of steady-state kinetics methods can also be employed to further analyze whether **I** and I_{th} are indeed the same transient species, i.e., whether mechanistic information obtained for **I** is indeed relevant to the thermal reaction.

2. Possible intermediates

Before summarizing individual systems, one might try to anticipate what types of intermediates would be generated as the result of the flash photoexcitation of the parent acetyl complexes such as $CpFe(CO)_2(COCH_3)$ or $Mn(CO)_5(COCH_3)$. The initial excitation (probably giving ligand field excited states) leads to CO dissociation at a rate too fast to observe directly from the excited state using the fastest time resolution (10 ns) of our present systems. Some methyl–metal bond fragmentation is apparent from the products as also is some "prompt" formation of the methyl complexes at a rate also too fast to observe directly with the ns equipment. Nonetheless, the principal photoprocess observed is CO dissociation to give **I**, and the nature of the time-resolved experiments, especially TRIR, allows one to follow subsequent reactions of **I** without interference from other pathways.

What form might **I** take? Fig. 1 depicts some alternatives, notably, the fully unsaturated species **U**, the chelated structure **C** with an η^2-carbonyl group, the solvated intermediate **S** and the bidentate transient **B** with the methyl group in an agostic interaction with the metal center. A truly coordinatively unsaturated intermediate (**U**) of a d^6 metal center such as Fe(II) or Mn(I) seems quite unlikely to be seen on the ns to ms time scales of most flash experiments. Earlier workers have

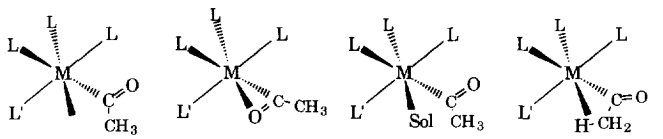

Fig. 1. Possible structures of **I** generated by flash photodissociation of a ligand from an acyl complex.

demonstrated that $Cr(CO)_5$ and its Mo and W pentacarbonyl homologs, as well as other analogous species, bind alkanes with dissociation energies as large as 10 kcal mol^{-1} and bind better donor ligands much more strongly [29,30]. Thus, we will generally not consider that alternative as likely to be observable in the solvent media described here. In the same context, therefore, the solvento species **S** must be given serious attention as a possible candidate for **I**, not only in strongly donor media but also in hydrocarbon solvents. If L and/or L′ are carbonyls, the frequencies of the ν_{CO} bands will provide a fairly sensitive probe of the electronic environment around the metal center. Thus, for **S**, these should shift to lower frequencies as the donor strength of the solvent increases. Furthermore, the lability of **S** in subsequent reactions with other ligands including CO should be especially sensitive to the solvent donicity. Data will be presented for other complexes which might serve as models for **S** which further support that contention. Although none of the spectra or kinetics of the species described here are likely to find the bulk solvent a totally innocent player, our contention is that spectral properties of the chelated species **C** or **B** should be but modestly solvent sensitive.In the absence of a better spectroscopic probe, it is necessary to fall back onto theoretical calculations to differentiate the relative viabilities of **C** and **B**. Earlier calculations [31–33] clearly point to **C** having the significantly lower energy. However, this conclusion must be moderated by NMR evidence in the case of the complex $Mo(S_2CX)(CO)(PMe_3)_2(COCH_3)$ ($X=NR_2$, OR) which has been used to argue for an equilibrium between agostic and η^2-CO species [34].

3. Studies of the intermediate $CpFe(CO)(COCH_3)$

This intermediate ($\mathbf{I_{Fe}}$) was prepared by 308 nm flash photolysis of the dicarbonyl complex $CpFe(CO)_2(COCH_3)$ ($\mathbf{A_{Fe}}$) (Eq. (3)) [35–37]. We have systematically probed the spectra and reactivity of $\mathbf{I_{Fe}}$ in various solvents and in the presence of various ligands.

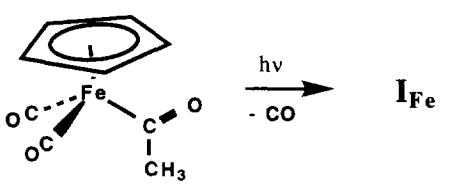

(3)

3.1. Transient spectra

TRIR spectra collected at ambient temperatures agreed with those at low-temperature FTIR in similar solvents, although the acyl ν_{CO} absorbances were difficult to detect with TRIR. Comparisons of how the spectra of $\mathbf{A}_{Fe}$ and $\mathbf{I}_{Fe}$ respond to solvent media of varying donor abilities provide some insight regarding the nature of the coordination of the site labilized by CO photodissociation. The terminal ν_{CO} band for $\mathbf{I}_{Fe}$ was detected at 1949 cm^{-1} in alkane solvents and at 1959 cm^{-1} in perfluoromethylcyclohexane (see Table 1). However, since analogous 10-cm^{-1} differences were observed in the IR spectra of $\mathbf{A}_{Fe}$, the differences may be the result of global effects on the spectra rather than of direct solvent coordination. The situation is clearer in the more strongly donating solvents such as THF, 2-Me THF and ACN, where ν_{CO} positions for $\mathbf{A}_{Fe}$ are similar to that in cyclohexane, yet the transient IR spectra for $\mathbf{I}_{Fe}$ exhibit significant ($\sim$30 cm^{-1}) shifts of the ν_{CO} to lower frequencies [35]. Direct solvent–metal coordination as in **S** is consistent with these results in donor solvents; but the spectral data for $\mathbf{I}_{Fe}$ in alkanes and perfluoroalkanes remain enigmatic.

As stated above, acyl ν_{CO} bands of $\mathbf{I}_{Fe}$ were difficult to detect via room-temperature TRIR spectroscopy; however, they were observable by FTIR detection following laser flash photolysis of $\mathbf{A}_{Fe}$ in −78°C glassy solutions. The acyl absorbs at 1585 cm^{-1} in methylcyclohexane and at 1611 cm^{-1} in 2-Me THF. Lower acyl ν_{CO} values have been attributed to η^2-acyl coordination to the metal center [38,39]. The 26-cm^{-1} difference in these two solvents would therefore be consistent with the η^2-acyl structure **C** existing in methylcyclohexane, and the η^1-acyl solvento **S** in 2-Me THF. Earlier studies have suggested solvent assistance in the carbonylation of $CpFe(CO)_2CH_3$ in THF but not in hexane [24].

3.2. Reactivities

Kinetic parameters have also been determined for competing reactions of $\mathbf{I}_{Fe}$ in various environments. The intermediate may undergo methyl migration to form

Table 1
Spectral data for $CpFe(CO)_2(COCH_3)$ ($\mathbf{A}_{Fe}$) and $CpFe(CO)(COCH_3)$ ($\mathbf{I}_{Fe}$) determined by TRIR (22°C) and FTIR (−78°C) spectroscopy; rate constants k_M (methyl migration) and k_L (L=$P(OCH_3)_3$) at 22°C under argon

Solvent	$\nu_{co}(A_{Fe})$ (cm^{-1})	$\nu_{CO}(I_{Fe})$ (cm^{-1})	k_M (s^{-1})	k_L ($M^{-1}s^{-1}$)
PFMC	2025, 1969, 1676	1959	9.4×10^4	1.4×10^7
c-Hexane	2018, 1963, 1669	1949	6.1×10^4	3.7×10^6
Isooctane	2018, 1963, 1670	1949	4.0×10^4	–
2-Me THF	2016, 1955, 1659	1922	3.9×10^4	2.5×10^5
THF	2015, 1955. 1658	1921	5.6×10^3	2.6×10^4
MCH[a,b]	2023/2018, 1968/1962, 1670/1627	1936, 1585		–
2-Me THF[b]	2013, 1958, 1656	1917, 1611	–	–

[a]MCH = methylcyclohexane; [b]$T=-78$°C.

$CpFe(CO)_2CH_3$ ($\mathbf{M_{Fe}}$) ($\Phi = 0.62$ mol einstein^{-1} in the solvents studied) or ligand trapping to form $CpFe(CO)L(COCH_3)$ in the presence of a nucleophile L (Eq. (4)). P_{CO} up to 1 atm ([CO] ~ 0.01 M), does not affect methyl migration quantum yields or rates. Thus recombination with CO does not effectively compete with methyl migration, and only the upper limit for k_{CO} (6×10^5 M^{-1} s^{-1} in cyclohexane) was estimated [35]. $\mathbf{I_{Fe}}$ was observed to be more reactive toward better Lewis bases such as PR_3, so direct competition of ligand substitution with methyl migration could be studied for such ligands.

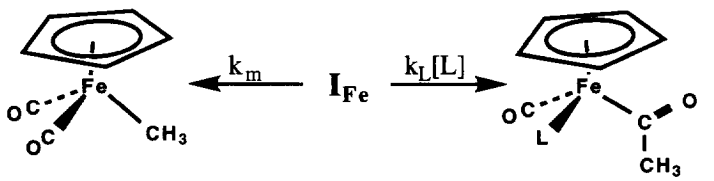

(4)

A modest solvent dependence on the migration rate constant k_M was observed (see Table 1). In contrast to the manganese complexes described below, k_M is faster in PFMC than in cyclohexane. A larger (though not pronounced) range of values was observed for k_L. The k_L for reaction of $\mathbf{I_{Fe}}$ with $P(OMe)_3$ in PFMC was but 4× that in cyclohexane. If $\mathbf{I_{Fe}}$ were the solvento species **S**, a much greater effect might be expected. For example, recombination of $Cr(CO)_5$ with CO is three orders of magnitude faster in PFMC than in cyclohexane [40]. Thus it is likely that $\mathbf{I_{Fe}}$ has a similar structure in both solvents, most likely **C** or **B**, with the spectroscopic data noted above favoring **C**. In the donor solvents, THF and 2-Me THF, stabilization from a solvent–metal interaction is supported by the significantly smaller k_L values. The seemingly anomalous differences between k_M and k_L values in 2-Me THF and in THF may be result from steric effects and is under further investigation.

From the kinetic and spectroscopic evidence described in the preceding sections, we have concluded that the solvento species **S** is present in solvents of significant donor ability, such as THF, but the η^2-acyl structure **C** dominates in lesser donating solvents, such as cyclohexane and PFMC.

3.3. *Mechanisms of* $\mathbf{I_{Fe}}$ *reactions*

In an earlier study [41] of pressure effects on the relative quantum yields of the methyl migration and $P(OMe)_3$ substitution pathways in *n*-heptane, it was found that higher pressures favor substitution over migration. Although absolute quantum yields were not measured, the ratio between the competing processes was used to calculate the difference between the activation volumes ($\Delta V^{\ddagger}_m - \Delta V^{\ddagger}_L = 39$ cm^3 mol^{-1}). This large difference was attributed to the pathways proceeding via markedly different mechanisms. For example, the ligand substitution might occur associatively via a "ring slip" mechanism (i.e., $\eta^5 \rightarrow \eta^3 \rightarrow \eta^5$), and the migration process via a mechanism having a much more dissociative character.A test of ring slip mechanisms is to compare the kinetics of cyclopentadienyl complexes with their

indenyl analogs, since the latter exhibit enhanced associative ligand substitution rates (the "indenyl effect") [42]. Accordingly, TRIR studies were carried out on the reaction of the photochemically generated indenyl acetyl intermediate (Ind)Fe(CO)$_2$(COCH$_3$) (Ind = η^5-C$_9$H$_7$) with L = CO, PPh$_3$ and P(OCH$_3$)$_3$. The TRIR spectrum of flash photolyzed (Ind)Fe(CO)$_2$(COCH$_3$) (Fig. 2) proved to be similar to that for $\mathbf{I}_{Fe}$, with one terminal ν_{CO}. There was no evidence for a dicarbonyl transient such as (η^3-Ind)Fe(CO)$_2$(COCH$_3$) or (η^3-Ind)Fe(CO)$_2$(COCH$_3$)L. Low temperature FTIR spectra of the indenyl transient agree well with that seen with ambient temperature TRIR. Furthermore the reactivities of $\mathbf{I}_{Fe}$ and its indenyl analog towards these ligands proved to be quite similar (Table 2), which is a further indication that trapping by these ligands *does not* occur via a ring slip mechanism. These results are consistent with investigations by Bassetti [43] and Cutler [44], in which thermal CO insertion reactions of the indenyl methyl compound (Ind)Fe(CO)$_2$CH$_3$ were studied and interpreted as not supporting the ring slip mechanism.Concerted associative attack of P(OCH$_3$)$_3$ on $\mathbf{I}_{Fe}$ (presumed to be the η^2-acyl coordinated species in hexane) should display a negative $\Delta V_L^{\ddagger}$. For the associative reactions of CpRh(CO)$_2$ with PPh$_3$ and P(*n*-Bu)$_3$ in toluene, activation volumes of -14 and -17 cm^{-3} mol^{-1} were measured [45]. Accordingly, given the

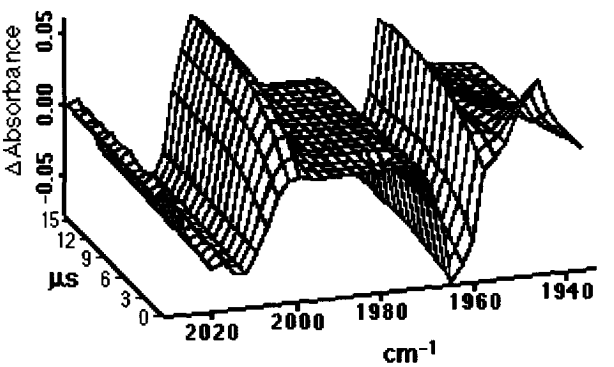

Fig. 2. IR spectral changes at 1-μs intervals following 308-nm flash photolysis of (Ind)Fe(CO)$_2$(COCH$_3$) (cyclohexane, Ar, 25°C).

Table 2
Kinetic studies on CpFe(CO)(COCH$_3$) and (Ind)Fe(CO)(COCH$_3$) with TRIR spectroscopy (cylclohexane, Ar, 22°C except where noted)

I	L	k_M (s^{-1})	k_L (M^{-1} s^{-1})
CpFe(CO)(COCH$_3$)	CO	5.7×10^4	$< 6 \times 10^6$
	P(OCH$_3$)$_3$	6.1×10^4	3.7×10^6
	PPh$_3$	5.6×10^4	2.4×10^6
(Ind)Fe(CO)(COCH$_3$)	CO	2.8×10^5	$< 3 \times 10^6$
	P(OCH$_3$)$_3$(27°)	3.6×10^5	2.1×10^7
	PPh$_3$	2.8×10^5	1.2×10^7

39 cm^{-3} mol^{-1} difference between k_M and k_L paths, the former must have a positive activation volume. Unimolecular methyl migration from an η^2-chelated acyl group as in **C** to give $\mathbf{M_{Fe}}$ must involve considerable rearrangement before the CH_3 group can move from the acetyl group to the metal. For example, one might suggest that the oxygen of the η^2-acyl chelate first dissociates, then the acetyl group rotates to a configuration more favorable for methyl migration. Since this reaction is faster in the very weakly coordinating perfluoro solvent PFMC than in cyclohexane, it must not be significantly solvent assisted and can be envisioned as having a positive $\Delta V^{\ddagger}_{m}$. Thus, in cyclohexane it appears that $\mathbf{I_{Fe}}$ reacts with L to form the substituted acetyl complex via an associative bimolecular mechanism in competition with a dissociative process leading to intramolecular methyl migration. These proposals are depicted in Scheme 1.

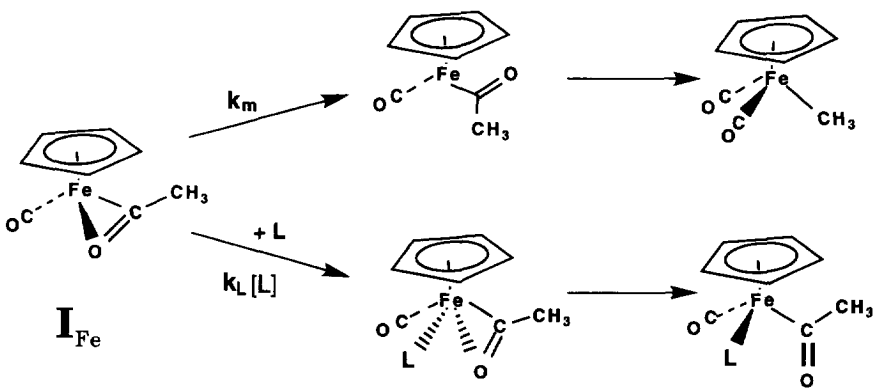

Scheme 1

4. The carbonylation of $Mn(CO)_5CH_3$

By the same methodology as employed in the study of the iron system, structural and mechanistic information about the "unsaturated" intermediate in the carbonylation of $Mn(CO)_5CH_3$ ($\mathbf{M_{Mn}}$) can be obtained using TRIR and TRO spectroscopies. In this case, photochemical decarbonylation of the acetyl complex $Mn(CO)_5(COCH_3)$ ($\mathbf{A_{Mn}}$) [3,6] results in formation of an intermediate ($\mathbf{I_{Mn}}$) which can undergo methyl migration to form $\mathbf{M_{Mn}}$ (Eq. (2)), recombination with CO to return to $\mathbf{A_{Mn}}$, or trapping with a different L to form complexes of the type *cis*-$Mn(CO)_4(L)(COCH_3)$.The effect of solvent on the rates of both the migration and substitution reactions of $\mathbf{I_{Mn}}$ (as determined by fast spectroscopic techniques, TRIR, TRO) allows us to elucidate its structure and determine the mechanism of the migration process. When combined with complementary studies of the thermal carbonylation reaction (i.e., the forward reaction, Eq. (1)), we can demonstrate that the photochemically generated intermediate is that produced in the thermal carbonylation reaction, allowing us to determine the reaction coordinate for the entire

migration process.We begin by showing that our photochemical scheme described in Eq. (2) is in fact valid. Continuous wave photolysis (313 nm) of $\mathbf{A_{Mn}}$ at room temperature in various organic solvents results in formation of $\mathbf{M_{Mn}}$ with good photochemical efficiency under argon ($\Phi = 0.62$), and the reaction is inhibited by added CO in accord with Eq. (2). The intermediate in the photochemical reaction was observed in the TRIR experiment: XeCl (308 nm) excimer photolysis of $\mathbf{A_{Mn}}$ in organic solvents resulted in depletion of $\mathbf{A_{Mn}}$ (IR: 2113(w), 2051(m), 2012(s), 1661(w) cm^{-1}) and prompt (<150 ns) formation of an intermediate (Fig. 2) with IR absorbances different than those of $\mathbf{A_{Mn}}$ and $\mathbf{M_{Mn}}$. These bands are attributed to $\mathbf{I_{Mn}}$ and are listed in Table 3. The ν_{CO} bands for $\mathbf{I_{Mn}}$ are shifted to lower energy than those of $\mathbf{A_{Mn}}$ in all solvents, consistent with the removal of a π-acid ligand from the coordination sphere. A weak band was observed for the acyl group of $\mathbf{I_{Mn}}$ at ~1600 cm^{-1}, shifted ~60 cm^{-1} lower in energy than the parent. The IR spectra of $\mathbf{I_{Mn}}$ displayed a modest sensitivity to solvent. In contrast to the iron system, the transient generated displayed little reactivity over several hundred μs in all solvents investigated, even under CO (1 atm), although it eventually decayed to a mixture of $\mathbf{M_{Mn}}$ and $\mathbf{A_{Mn}}$. The relative stability of $\mathbf{I_{Mn}}$ allowed for its detection by FTIR following photolysis of $\mathbf{A_{Mn}}$ at −78°C, where the intermediate is stable indefinitely. Good agreement was observed between the low and room temperature experiments.$\mathbf{I_{Mn}}$ is much less reactive than other "unsaturated" intermediates derived from d^6 metal carbonyl complexes such as $Cr(CO)_6$, which exist as solvento species (**S**), even in weakly coordinating solvents. We therefore sought a model closely related to $\mathbf{A_{Mn}}$ but lacking the acyl functionality, so that we could confidently generate and interrogate the reactivity of a solvento intermediate, and use this as a benchmark for the reactivity of **S**. In this context, the time-resolved spectra and dynamics of transient species formed by the flash photolysis of $\mathbf{M_{Mn}}$ (Eq. (5)) were examined as the closest analog for $\mathbf{A_{Mn}}$ without the acyl function.

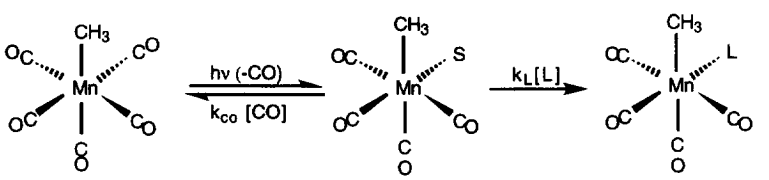

M **Z_{Mn}** **M_L** (5)

4.1. *Intermediate generated from $Mn(CO)_5CH_3$*

Before speculating on the reactivity of the different structures of $\mathbf{I_{Mn}}$, it is instructive to compare its reactivity to that of an intermediate generated when a suitable model is treated similarly [10]. Fig. 3 shows the TRIR spectra resulting from the flash photolysis of $\mathbf{M_{Mn}}$ in cyclohexane solution under CO. The notable features are the prompt formation of a transient $\mathbf{Z_{Mn}}$ which decays exponentially within a few μs, i.e., much faster than $\mathbf{I_{Mn}}$ under analogous conditions. A plot of k_{obs} vs. [CO] proved

Table 3
Carbonyl bands (ν_{CO} values in cm^{-1}) for $\mathbf{I_{Mn}}$ formed by 308-nm excitation of $\mathbf{A_{Mn}}$ in various solvents at ambient T and at 195 K as measured by TRIR and FTIR, respectively

Solvent	ν_{CO}	
	296 K[a]	195 K[b]
PFMC	1997, 1959	2083(w), 1998, 1958
Cyclohexane	1990, 1952, 1607(w)	
Methylcyclohexane	1990, 1952	2080(w), 1988, 1941, 1607(w)
Dichloromethane	1987 (br), 1940 (br)	
Toluene	1984 (br), 1941 (br)	
THF	1981 (br), 1931 (br)	2077(w), 1977, 1928, 1602(w)
2,2,5,5-Me_4THF	1984 (br), 1945 (br)	

[a]Ambient T data taken from TRIR spectra 100 ms after 308-nm flash excitation.
[b]Low T data recorded on a Bio-Rad FTS-60 FTIR spectrometer immediately after excitation.

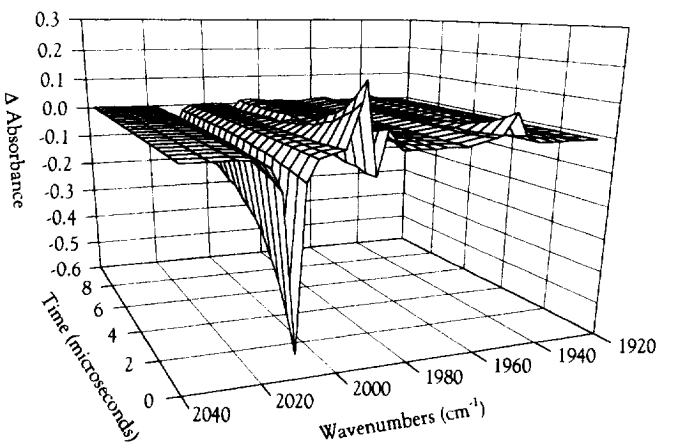

Fig. 3. Transient IR spectral changes following 308-nm laser flash photolysis of $Mn(CO)_5CH_3$ in 295 K cyclohexane under 10% CO (500-ns intervals).

to be linear with slope k_{CO} of $4.8 \times 10^8\ M^{-1}\ s^{-1}$. However, in a more strongly donating solvent such as THF, the rate of CO substitution was greatly reduced; $k_{CO} = 1.4 \times 10^2\ M^{-1}\ s^{-1}$. Similarly, the TRIR spectra of $\mathbf{Z_{Mn}}$ proved to be strongly dependent on medium (Table 4) with ν_{CO} bands shifted to lower frequencies for more electron donating solvents. This pattern is consistent with that shown above for $\mathbf{I_{Mn}}$ formed by the photolysis of $\mathbf{A_{Mn}}$ in the various solvents, but the magnitude of the spectral changes were larger for $\mathbf{Z_{Mn}}$. The dramatic solvent effects on the substitution reactivity and IR spectra of $\mathbf{Z_{Mn}}$ led us to conclude that this species is in fact is a solvento complex [10]. Effectively, we can now use the substitution reactivity of $\mathbf{Z_{Mn}}$ as a test for the existence of a solvento structure in the reactions of $\mathbf{I_{Mn}}$.

Table 4
The reactivity of $\mathbf{I}_{Mn}$ with L in cyclohexane, PFMC and THF: comparison of the reactivity of $\mathbf{I}_{Mn}$ vs. that of the $CH_3Mn(CO)_4(Sol)$ analog

Solvent	Ligand	k_L ($M^{-1}s^{-1}$)	
		$\mathbf{I}_{Mn}$[a]	$\mathbf{Z}_{Mn}$[b]
Cyclohexane	Phpy	$(7.5\pm1.5)\times10^6$	$(2.5\pm0.3)\times10^9$
Cyclohexane	$P(Ph)_3$	$(2.3\pm0.5)\times10^6$	$(1.0\pm0.2)\times10^9$
Cyclohexane	$P(OMe)_3$	$(1.4\pm0.3)\times10^6$	$(1.1\pm0.2)\times10^9$
THF	$P(OMe)_3$	$(1.7\pm0.3)\times10^3$	
2,2,5,5-Me_4THF	$P(OMe)_3$	6×10^5	
Cyclohexane	CO	$(6.5\pm1.3)\times10^3$	$(4.5\pm0.5)\times10^8$
PFMC	CO	$(1.5\pm0.3)\times10^4$	$(1.0\pm0.5)\times10^{10}$
THF	CO	$<5\times10^2$	$(1.4\pm0.3)\times10^2$

[a]Ref. 3; [b]Ref. 10.

4.2. *The Structure of* $\mathbf{I}_{Mn}$

We have concluded previously that the profound effect of solvent on the substitution reactivity and spectra of $\mathbf{Z}_{Mn}$ are most consistent with its formulation as a solvent coordinated species. It is instructive to compare the rates of ligand substitution of $\mathbf{I}_{Mn}$ to those of $\mathbf{Z}_{Mn}$ in various solvents. For example the k_{CO} values obtained for $\mathbf{I}_{Mn}$ and $\mathbf{Z}_{Mn}$ in perfluoromethylcyclohexane were 1.5×10^4 and $1.0\times10^{10}\,M^{-1}s^{-1}$, respectively; however, the corresponding values in THF were $\sim4\times10^2$ and $1.4\times10^2\,M^{-1}s^{-1}$. The comparative sluggishness with which $\mathbf{I}_{Mn}$ undergoes ligand substitution in weakly coordinating solvents (Table 5) relative to $\mathbf{Z}_{Mn}$ suggests that $\mathbf{I}_{Mn}$ is not a solvento species (**S**) under such conditions. Two logical structures in which the acyl group can stabilize the intermediate are as an η^2 chelate illustrated by structure **C** and the agostically bound methyl group (**B**). In a previous study [3] we have shown that the spectral and kinetic data for $\mathbf{I}_{Mn}$ in weakly coordinating solvents are most consistent with the η^2 chelate **C**. However,

Table 5
Rate constants for CO addition (k_{CO}) and methyl migration (k_M) reactions of $\mathbf{I}_{Mn}$ in various solvents determined from optical flash photolysis experiments

Solvent	k_{CO}[a] ($M^{-1}s^{-1}$)	k_M (s^{-1})
PFMC	$(1.5\pm0.2)\times10^4$	<1.0
Benzene	$(3.3\pm0.3)\times10^3$	6.7 ± 0.7
Cyclohexane	$(6.5\pm0.7)\times10^3$	9.0 ± 0.9
Dichloromethane	$(5.3\pm0.5)\times10^3$	30.4 ± 3.0
1,2 Dichloroethane	$(7.3\pm0.7)\times10^3$	46.8 ± 4.7
THF	$<5\times10^2$	8.8 ± 1

[a]Concentrations of CO in various solvents were corrected for differences in solubility: IUPAC Solubility Data Series: Carbon Monoxide v. 43, R.W. Cargill (Ed.) Pergamon Press, New York, 1990.

in stronger donor solvents rates of ligand substitution are similar, suggesting that the intermediate is the solvento species, **S**.

4.3. Methyl migration

Having established the structure of $\mathbf{I}_{Mn}$ in various media, we turn to the effect of solvent on the rate of methyl migration, presumably the microscopic reverse of the first step in the thermal carbonylation reaction (see below). The k_M values in various solvents, determined by TRO spectroscopy both directly via the first order decay of $\mathbf{I}_{Mn}$ in the absence of added ligands and by competitive trapping experiments in accord with Eq. (2), are summarized in Table 3. Notably, the trends observed for k_M do not parallel those of the ligand substitution reactions. Although phosphine substitution of $\mathbf{I}_{Mn}$ is three orders of magnitude faster in cyclohexane than in THF, the rate of methyl migration was found to be nearly identical in the two solvents. The similar values for k_M in these solvents must be coincidental given the different $\mathbf{I}_{Mn}$ structures in the two solvents. Because k_L values are depressed, donor solvents therefore tend to favor methyl migration in the competitive reactions of $\mathbf{I}_{Mn}$.

Fig. 4 illustrates the role of the solvent in promoting methyl migration in a schematic free energy diagram. In weakly coordinating solvents (alkanes, aromatics, halocarbons), where $\mathbf{I}_{Mn}$ exists as the η^2 chelate, the solvent is nonetheless involved in the methyl migration step owing to the solvent dependence of k_M. Upon inspection of the η^2 acyl structure it is difficult to imagine a one-step process by which it could

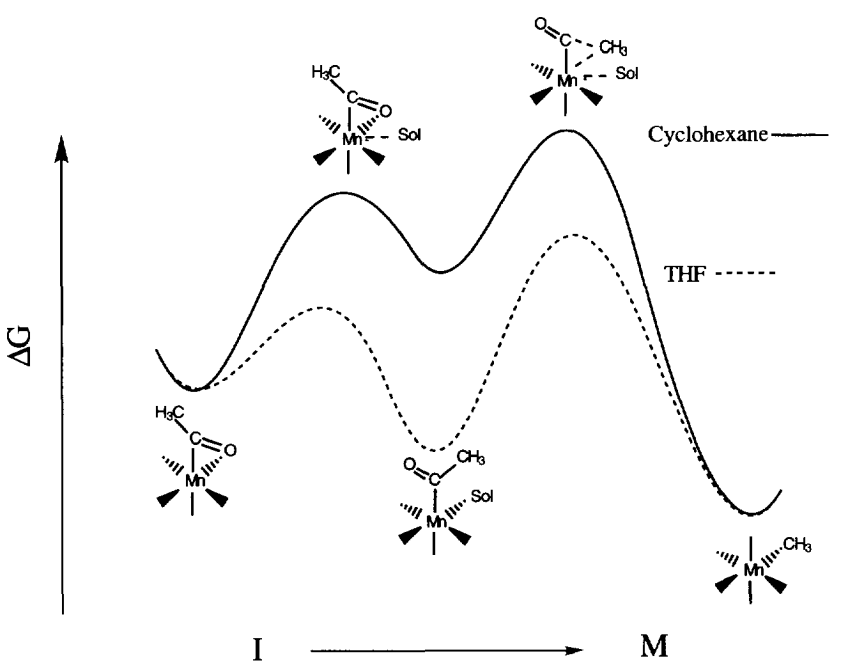

Fig. 4. Free energy profile for k_M pathway from $\mathbf{I}_{Mn}$.

rearrange to $\mathbf{M}_{Mn}$. We propose that the trend of increasing k_M with donating ability of the solvent is the result of the η^2 chelate **C** reacting first to form the solvento species, which then undergoes methyl migration with concerted loss of solvent. This is the microscopic reverse of the previously proposed "solvent assisted" methyl migration. Furthermore, the substitution of the coordination site occupied by the acyl oxygen with a solvent molecule followed by methyl migration to the same site is consistent with the stereochemical observations made for the reverse reaction. In THF, the lowest energy form of $\mathbf{I}_{Mn}$ is already the solvento species **S**. Thus, stabilization of **S** by Mn–THF bonding offsets stabilization of the k_M transition state by solvent–metal interactions giving the fortuitous similarity of the $\Delta G^{\ddagger}_{in}$ values in cyclohexane and THF.

4.4. Comparison of the thermal and photochemical kinetics

After having established the structure and reactivity of $\mathbf{I}_{Mn}$ with respect to methyl migration a key question remains to be resolved: Is the photochemically generated intermediate the same as that produced in the thermal carbonylation reaction? If so, then the mechanistic information obtained for $\mathbf{I}_{Mn}$ can be used to interpret the thermal process. While data concerning solvent assistance in the above photochemical studies do qualitatively agree with previously observed thermal results, we can make a quantitative comparison of the reactivity of $\mathbf{I}_{Mn}$ and $\mathbf{I}_{Th}$. Specifically, if an intermediate shows the same branching selectivity between methyl migration and ligand substitution, whether it is produced thermally or photochemically, then the intermediate is likely to be the same.The reaction of $\mathbf{M}_{Mn}$ with $P(OMe)_3$ was investigated in order to provide comparative thermal and photochemical data under closely analogous conditions. Earlier kinetics studies [16] of reactions of $\mathbf{M}_{Mn}$ with other L to give the respective acetyl complexes *cis*-$\mathbf{A}_L$ in various solvents were interpreted in terms of the model illustrated in Scheme 2, which gives the relationship described by Eq. (6).

$$k_{obs} = \frac{k_1 k_2[L]}{k_{-1} + k_2[L]} + k_3[L] \tag{6}$$

In THF, the $k_3[L]$ term for direct reaction of L with $\mathbf{M}_{Mn}$ is small, and values of k_1 as well as the ratio k_{-1}/k_2 can be obtained for various L from the slopes and intercepts of double reciprocal k_{obs}^{-1} vs. $[L]^{-1}$ plots. Indeed, the reaction of $\mathbf{M}_{Mn}$ with excess $P(OMe)_3$ in THF to give *cis*-$CH_3C(O)Mn(CO)_4(P(OMe)_3)$ followed pseudo first-order kinetics at all $P(OMe)_3$ concentrations. From the linear plot of k_{obs}^{-1} vs. $[L]^{-1}$ were determined $k_1 = (8.5 \pm 0.9) \times 10^{-4}\ s^{-1}$ and $k_{-1}/k_2 = (6.6 \pm 1.3) \times 10^{-3}$ M. If $\mathbf{I}_{Mn}$ identified by the photochemical techniques is indeed the same as the thermal intermediate $\mathbf{I}_{th}$, these two species must have identical reactivities regardless of how they were individually generated. If $\mathbf{I}_{Mn}$ and $\mathbf{I}_{th}$ are the same, then k_M is k_{-1} and k_L is k_2; therefore, k_M/k_L and k_{-1}/k_2 should be equal. The photochemical experiment allows one to determine k_M and k_L independently. The calculated k_M/k_L ratio is $(5.5 \pm 1.5) \times 10^{-3}$ M, within experimental uncertainty the same as k_{-1}/k_2. Thus, the

assertion that the photochemically generated intermediates are relevant to thermally induced migratory insertion is supported.

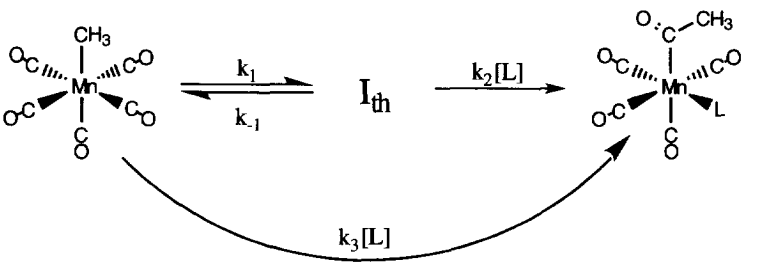

(6)

$$k_{obs} = \frac{k_1 k_2[L]}{k_{-1} + k_2[L]} + k_3[L]$$

Scheme 2

Thus, having established that the photochemical intermediate is the same as that in the thermochemistry, the kinetic information obtained for $\mathbf{I}_{Mn}$ can be combined with the kinetics and thermodynamics of the thermal reaction to describe the complete reaction coordinate in terms of free energy. In Fig. 5 are plotted free energy changes for the reaction of $\mathbf{M}_{Mn}$ in THF with 0.1 M $P(OMe)_3$.

5. Studies of cobalt–carbonyl systems

Having demonstrated the utility of this approach in understanding the mechanisms of the carbonylations of model complexes, we are applying this technique to catalytically active systems. Hydroformylation catalysts derived from $Co_2(CO)_8$/phosphine precursors have long been used in the industrial production of aldehydes [11]. Complexes such as $Co(CO)_3(L)R$ (R = hydride, alkyl, acyl) have all been proposed as meta-stable intermediates in the hydroformylation cycle. We should be able to prepare the reactive fragments from these species and interrogate their reactivity using the same approach as in the model complexes.

thermal:

$$M \underset{k_{-1}}{\overset{k_1}{\rightleftharpoons}} I_{th} \xrightarrow{k_2[L]} A_L$$

photochemical:

$$M \xleftarrow{k_M} I \underset{k_L[L]}{\overset{h\nu, -CO}{\rightleftharpoons}} A_L$$

Information such as absolute reaction rates of intermediates with different ligands would be invaluable in the design of catalytic systems. For example, a measure of the reactivities of an intermediate with H_2, CO, and olefin would be important to a hydroformylation catalyst.We are carrying out preliminary experiments

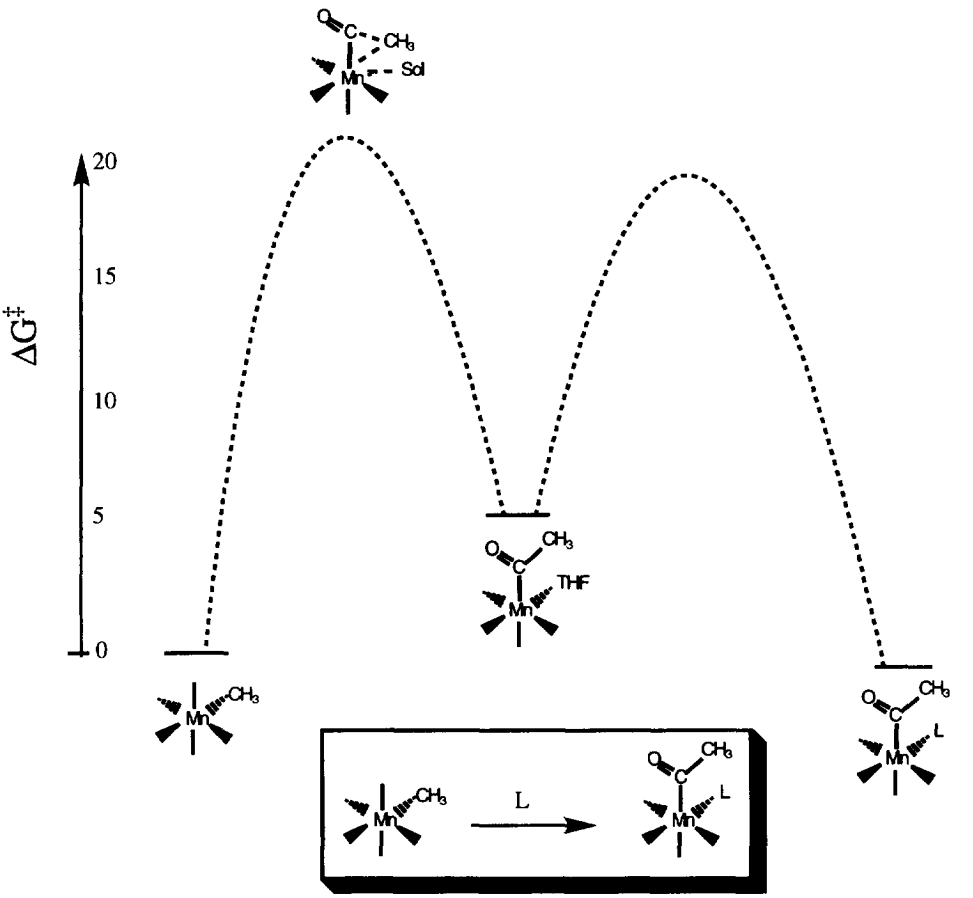

Fig. 5. Free energy profile for the carbonylation at 25°C with 0.1 M $P(OMe)_3$.

on the reactivity of intermediates generated from photolysis of $Co(CO)_3(PPh_3)(COCH_3)$ ($\mathbf{A}_{Co}$). Continuous wave photolysis of $\mathbf{A}_{Co}$ in room temperature organic solvents results in formation of $Co(CO)_3(PPh_3)CH_3$ ($\mathbf{M}_{Co}$) with good efficiency. Flash photolysis of $\mathbf{A}_{Co}$ in CH_2Cl_2 with TRIR detection leads to observation of intermediate $\mathbf{I}_{Co}$ with spectral characteristics consistent with its formulation as resulting from CO photoejection. $\mathbf{I}_{Co}$ rearranges very rapidly to $\mathbf{M}_{Co}$ ($k_M = 2.0 \times 10^5\ s^{-1}$). In THF, the analogous reaction is faster ($1.1 \times 11^6\ s^{-1}$). We are currently adapting our sample handling equipment to accommodate the high gas pressures required to generate many of the species in the cobalt system.

6. Summary

We have demonstrated that when employed in a rigorous mechanistic study of an organometallic reaction, TRIR and TRO spectroscopies provide valuable, otherwise

unobtainable, structural and kinetic information about intermediates in the reaction sequence. In particular, we have used this technique to determine the structure and reactivity of such species in the carbonylations of $CpFe(CO)_2CH_3$ and $Mn(CO)_5CH_3$. In both cases, in weakly coordinating solvents the intermediate is stabilized intramolecularly, presumably via η^2 chelation, and in strong donor solvents the solvento species predominates. In the manganese case, the methyl migration step is found to involve concerted migration of the methyl group and formation of an Mn–solvent bond, irrespective of the most stable structure of $\mathbf{I}_{Mn}$. In contrast, the role of solvent is apparently much less important in defining the rates of the migratory pathways in the cyclopentadienyl iron analogs. These techniques are now in the process of being adapted to the study of an active hydroformylation catalyst.

Acknowledgements

This research was sponsored by a grant (DE-FG03-85ER13317) to PCF from the Division of Chemical Sciences, Office of Basic Energy Sciences, US Department of Energy. Some laser flash photolysis experiments were carried out on a time resolved optical system constructed with support from a US Department of Energy University Research Instrumentation Grant (No. DE-FG05-91ER79039).

References

[1] P.C. Ford, W. Boese, B. Lee and K.L. McFarlane, Photocatalysis involving metal carbonyls, in M. Graetzel and K. Kalyanasundaram (eds.), Photosensitization and Photocatalysis by Inorganic and Organometallic Compounds, Kluwer Academic Publishers, The Netherlands, 1993, pp. 359–390 and Refs. therein.
[2] G. Henrici-Olivé and S. Olivé, Catalyzed Hydrogenation of Carbon Monoxide, Springer-Verlag, Berlin, 1984.
[3] W.T. Boese and P.C. Ford, J. Am. Chem. Soc., 117 (1995) 8381–8391.
[4] D.A. Wink and P.C. Ford, J. Am. Chem. Soc., 109 (1987) 436–442.
[5] P.C. Ford, T.L. Netzel, C.T. Spillet and D.B. Pourreau, Pure Appl. Chem., 62 (1990) 1091–1094.
[6] W.T. Boese, B.L. Lee, D.W. Ryba, S.T. Belt and P.C. Ford, Organometallics, 12 (1993) 4739–4741.
[7] A.J. Dixon, M.A. Healy, P.M. Hodges, B.D. Moore, M. Poliakoff, M.B. Simpson, J.J. Turner and M.A. West, J. Chem. Soc., Faraday Trans., 2(82) (1986) 2083–2092.
[8] S.P. Church, H. Herman, F.-W. Grevels and K. Schaffner, Inorg. Chem., 24 (1985) 418–422.
[9] J.A. DiBenedetto, D.W. Ryba and P.C. Ford, Inorg. Chem., 28 (1989) 3503–3507.
[10] W.T. Boese and P.C. Ford, Organometallics, 13 (1994) 3525–3531.
[11] G.W. Parshall and S.D. Ittle, Homogeneous Catalysis, Ch. 5, 2nd Edn., Wiley-Interscience, New York, 1992.
[12] J.P. Collman, L.S. Hegedus, J.R. Norton and R.G. Finke, Principles and Applications of Organotransition Metal Chemistry, Ch. 6, University Science Books, Mill Valley, CA, 1987.
[13] A. Wojcicki, Adv. Organomet. Chem., 11 (1973) 87–145.
[14] F. Calderazzo, Angew. Chem., Int. Edn. Engl., 16 (1977) 299–311.
[15] T.C. Flood, Top. Stereochem., 12 (1981) 37–118.
[16] R.J. Mawby, F. Basolo and R.G. Pearson, J. Am. Chem. Soc., 86 (1964) 3994–3999.

[17] T.C. Flood, J.E. Jensen and J.A. Statler, J. Am. Chem. Soc., 103 (1981) 4410.
[18] J.D. Cotton and T.L. Bent, Organometallics, 10 (1991) 3156–3160.
[19] J.N. Cawse, R.A. Fiato and R.L. Pruett, J. Organomet. Chem., 172 (1979) 405–413.
[20] S. Webb, C. Giandomenico and J. Halpern, J. Am. Chem. Soc., 108 (1986) 345–347.
[21] M. Green, R.I. Hancock and D.C. Wood, J. Chem. Soc. (A), (1968) 2718–2721.
[22] I. Butler, F. Basolo and R.G. Pearson, Inorg. Chem., 6 (1967) 2074–2079.
[23] M. Green and D.J. Westlake, J. Chem. Soc. (A), (1971) 367–371.
[24] J. Bibler and A. Wojcicki, Inorg. Chem., 5 (1966) 889–892.
[25] K. Nicholas, S. Raghu and M. Rosenblum, J. Organomet. Chem., 78 (1974) 133–137.
[26] J.D. Cotton, G.T. Crisp and L. Latif, Inorg. Chim. Acta, 47 (1981) 171–176.
[27] K.D. Campbell and T.C. Flood, J. Am. Chem. Soc., 106 (1984) 2853–2860.
[28] T.C. Forschner and A.R. Cutler, J. Organomet. Chem., (1989) 361.
[29] G.K. Yang, V. Vaida and K.S. Peters, Polyhedron, 7 (1988) 1619–1622.
[30] J. Morse, G. Parker and T.J. Burkey, Organometallics, 8 (1989) 2471–2474.
[31] F.U. Axe and D.S. Marynick, Organometallics, 6 (1987) 572–580.
[32] F.U. Axe and D.S. Marynick, J. Am. Chem. Soc., 110 (1988) 3728–3734.
[33] T. Ziegler, L. Verluis and V. Tscinke, J. Am. Chem. Soc., 108 (1986) 612–617.
[34] E. Carmona, L. Contreras, M.L. Poveda and L.J. Sánchez, J. Am. Chem. Soc., 113 (1991) 4322–4324.
[35] S.T. Belt, D.W. Ryba and P.C. Ford, J. Am. Chem. Soc., 113 (1991) 9524–9528.
[36] K.L. McFarlane and P.C. Ford, Manuscript in preparation.
[37] T.M. McHugh and A.J. Rest, J. Chem. Soc., Dalton Trans., (1980) 2323–2332.
[38] L.D. Durfee and I.P. Rothwell, Chem. Rev., 88 (1988) 1059–1079.
[39] R.L. Sweany, Organometallics, 8 (1989) 175–179.
[40] R. Bonneau and J.M. Kelly, J. Am. Chem. Soc., 102 (1980) 1220–1221.
[41] D.W. Ryba, R. van Eldik and P.C. Ford, Organometallics, 12 (1993) 104–107.
[42] M.E. Rerek and F. Basolo, Polyhedron, 9 (1990) 1503–1535.
[43] D. Monti and M.J. Bassetti, Am. Chem. Soc., 115 (1993) 4658–4664.
[44] T.C. Forschner and A.R. Cutler, J. Organomet. Chem., (1989) 361.
[45] P. Vest, J. Anhaus, H.C. Bajaj and R. van Eldik, Organometallics, 10 (1991) 818–819.